Received: 2 June 2021 | Revised: 29 June 2021 | Accepted: 29 June 2021

DOI: 10.1111/joa.13513

Journal of Anatomy ANATOMICAL SOCIETY WILEY

ORIGINAL PAPER

Paleobiological reconstructions of articular function require all six degrees of freedom

Armita R. Manafzadeh | **Stephen M. Gatesy**

Department of Ecology, Evolution, and Organismal Biology, Brown University, Providence, RI, USA

Correspondence
Armita R. Manafzadeh, Department of Ecology,Evolution, and Organismal Biology, Brown University, Providence, RI 02912, USA.
Email: armita_manafzadeh@brown.edu

Funding information
Society of Vertebrate Paleontology; Sigma Xi; Brown University; Association for Women Geoscientists/Paleontological Society; Bushnell Research and Education Fund; US National Science Foundation, Grant/Award Number: IOS-0925077, DBI-0552051, IOS-0840950, DBI-1262156 and EAR-1452119

Abstract

Paleobiologists typically exclude impossible joint poses from reconstructions of extinct animals by estimating the rotational range of motion (ROM) of fossil joints. However, this ubiquitous practice carries the assumption that osteological estimates of ROM consistently overestimate true joint mobility. Because studies founded on ROM-based exclusion have contributed substantially to our understanding of functional and locomotor evolution, it is critical that this assumption be tested. Here, we evaluate whether ROM-based exclusion is, as currently implemented, a reliable strategy. We measured the true mobilities of five intact cadaveric joints using marker-based X-ray Reconstruction of Moving Morphology and compared them to virtual osteological estimates of ROM made allowing (a) only all three rotational, (b) all three rotational and one translational, and (c) all three rotational and all three translational degrees of freedom. We found that allowing combinations of motions in all six degrees of freedom is necessary to ensure that true mobility is always successfully captured. In other words, failing to include joint translations in ROM analyses results in the erroneous exclusion of many joint poses that are possible in life. We therefore suggest that the functional and evolutionary conclusions of existing paleobiological reconstructions may be weakened or even overturned when all six degrees of freedom are considered. We offer an expanded methodological framework for virtual ROM estimation including joint translations and outline recommendations for future ROM-based exclusion studies.

KEYWORDS
joint mobility, joint translations, range of motion, vertebrate paleontology, XROMM

1 | INTRODUCTION

Reconstructions of organismal function have long been among the most common and broadly compelling pursuits of vertebrate paleobiology (see Thomason, 1995). Traditionally, paleobiologists began these reconstructions by physically manipulating pairs of fossil bones to estimate the rotational range of motion (ROM) of individual joints (e.g., Bramwell & Whitfield, 1974; Carpenter, 2002; Carpenter & Wilson, 2008; Fröbisch, 2006; Jenkins, 1971; Padian, 1983; Paul & Christiansen, 2000; Senter & Robins, 2005; Senter & Sullivan, 2019). Although virtual ROM analyses have largely superseded physical ones (e.g., Demuth et al., 2020; Mallison, 2010a,b; Molnar et al., 2021; Nyakatura et al., 2015, 2019; Pierce et al., 2012; Richards et al., 2021), their primary objective has remained the same: to identify impossible joint poses and to exclude potential behaviors that require them.

Paleobiologists generally defend ROM-based exclusion as a tenable—or even conservative—approach to functional reconstruction

because studies have indicated that osteological manipulations tend to overpredict true rotational ROM, and that only a subset of each joint's mobility is used in life (e.g., Arnold et al., 2014; Hutson & Hutson, 2012, 2013; Kambic et al., 2017a; Manafzadeh et al., 2021; Manafzadeh & Padian, 2018). By contrast, however, other analyses have concluded that osteological manipulations might actually underpredict true rotational ROM (e.g., Hutson & Hutson, 2014, 2015). If viable joint poses were to be omitted from ROM estimates, they would also erroneously be excluded from reconstructions before functional variables such as bone strain, energy expenditure, muscle moment arms, or balance (e.g., Bishop et al., 2021; Carrano et al., 1998; Molnar et al., 2021; Nyakatura et al., 2019) are even considered. This possibility is especially concerning because ROM-based exclusion of limb configurations has played a large role in shaping not only our understanding of the stance and gait of individual taxa (e.g., Gatesy et al., 2009; Lai et al., 2018; Mallison, 2010a,b; Richards et al., 2021) but also that of major transformations in locomotor evolution (such as the origins of terrestriality, bipedality, and flight; e.g., Demuth et al., 2020; Molnar et al., 2021; Nyakatura et al., 2019; Pierce et al., 2012).

In this study, we aimed to evaluate whether ROM-based exclusion is, as currently implemented, a reliable strategy for use in paleobiological reconstructions. Paleobiologists' approaches to virtual ROM analysis have varied substantially, ranging from manual exploration of joint configurations to an automated, exhaustive sampling of rotational pose space, but none to date have systematically allowed combinations of motions in all six degrees of freedom (both rotational and translational; Figure 1). Here, we tested how many degrees of freedom must be considered to ensure that all the poses in a joint's true mobility are consistently captured. To do so, we collected data from five joints that display a variety of morphologies. We first measured the true mobility of each joint from cadaveric manipulations using marker-based X-ray Reconstruction of Moving Morphology (XROMM; Brainerd et al., 2010; Manafzadeh, 2020). We then compared these mobilities to virtual, osteological estimates of ROM while allowing (a) only all three rotational, (b) all three rotational and one translational, and (c) all three rotational and all three translational degrees of freedom. Here, we present the results of this comparison and discuss their implications for existing functional reconstructions. Ultimately, we offer an expanded framework for virtual ROM estimation and outline recommendations for future ROM-based exclusion studies.

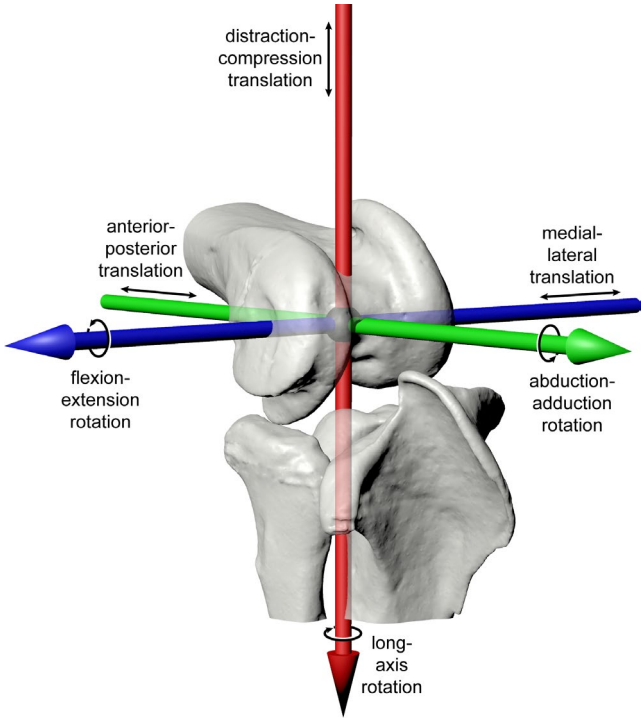

FIGURE 1 Joints have three rotational and three translational degrees of freedom. Degrees of freedom indicated by black arrows around and along colored axes for a right guineafowl knee joint (femur, tibiotarsus, and fibula) in anterolateral view. Red, green, and blue correspond to *X*, *Y*, and *Z* axes, respectively

2 | METHODS

2.1 | Cadaveric joint pose measurement

We first conducted a marker-based XROMM analysis of cadaveric manipulations (Brainerd et al., 2010; Manafzadeh, 2020) of Helmeted Guineafowl (*Numida meleagris*) and American alligator (*Alligator mississippiensis*) hindlimbs to measure the true passive mobility of the guineafowl hip, knee, and ankle and the alligator hip and knee. Detailed methods for this data collection were outlined by Manafzadeh et al., (2021); in this study, we include data from only one individual of each species to avoid minor inter-individual differences (see Kambic et al., 2017a; Manafzadeh & Padian, 2018) and allow direct comparison of results from real joint poses and virtual manipulations.

In short, the intact, marked left and right hindlimbs of each individual were manipulated within the calibrated X-ray volume created by two X-ray image systems recording synchronized video, with the goal of capturing all possible configurations of each hindlimb joint. Specimens were then disarticulated, and micro-computed tomography (micro-CT) scans were taken of all marked hindlimb elements. Coordinate systems (Grood & Suntay, 1983) and reference poses were generated for each individual in Maya 2020 (Autodesk), as by Manafzadeh et al., (2021) (largely following Kambic et al., [2014], Figure 2a,b). X-ray videos were calibrated and digitized using XMALab v. 1.5.4 (Knörlein et al., 2016), and the resulting rigid body transformations were used to animate bone models in Maya, where six degree-of-freedom joint kinematics were calculated using custom Maya Embedded Language scripts.

Previous XROMM studies have measured joint translations as the displacement of the distal anatomical coordinate system (ACS) origin relative to the proximal ACS origin along the axes of the proximal ACS (e.g., Camp & Brainerd, 2014; Dawson et al., 2011; Kambic et al., 2014; Menegaz et al., 2015). Although this approach provides

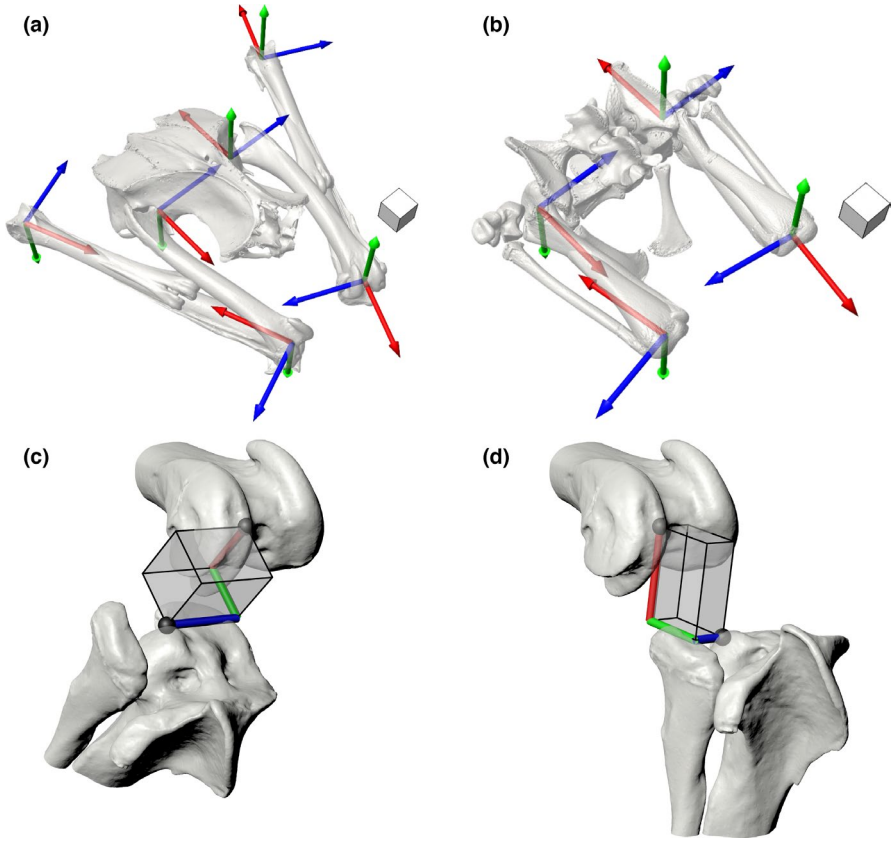

FIGURE 2 Measurement systems for joint kinematics. Joint coordinate systems in the reference pose (all rotations and translations equal zero) for the (a) Helmeted Guineafowl and (b) American alligator. Red, green, and blue correspond to *X*, *Y*, and *Z* axes, respectively. Scale cubes represent 1 cm. Prism-based hinge joint translation measurement system shown on a right guineafowl knee joint in anterolateral view (c) at flexion–extension rotation = 40 degrees with (*X*, *Y*, *Z*) translations = (0.8, 0.7, 1.0) cm and (*D*) at flexion–extension rotation = 80 degrees with (*X*, *Y*, *Z*) translations = (1.1, 0.8, −0.4) cm. Red, green, and blue cylinders reflect translations along *X*, *Y*, and *Z* axes, respectively; black spheres represent positions of the proximal and distal ACS origins. Note that the red *X* axis captures pure distraction–compression translation, and the green *Y* captures pure anterior–posterior translation, with separate degrees of freedom. See also Movie S1

a useful framework for studying ball and socket joints, which are not expected to be biased toward any single degree of freedom, it can be less effective for meaningfully characterizing the movements of "hinge-like" (hereafter hinge) joints, which are strongly dominated by a single rotational degree of freedom. Under the traditional convention, the anatomical consequences of X and Y translations change as hinge joints flex and extend about the Z axis. For example, when flexed at 90° (as in Figure 1), Y translation represents anterior–posterior sliding of the articular surfaces. However, when extended to 180°, Y translation instead represents joint distraction–compression, whereas X translation now measures anterior–posterior sliding. This inconsistency can make the communication of simple kinematic patterns, such as a fixed joint spacing measurement (i.e., fixed distraction–compression offset), unnecessarily complex.

Here, we instead aim to consistently partition hinge joint anterior–posterior and distraction–compression translations into two separate degrees of freedom, thus making our hinge joint (knee and ankle) translations more comparable to those measured from ball and socket (hip) joints. To do so, we establish a new set of axes that are best visualized using a rectangular prism, built holding the proximal and distal ACS origins at two diagonal vertices (Figure 2c,d; Movie S1). This prism rotates about its Z axis as the hinge joint rotates about the *Z* axis of its joint coordinate system, in effect mapping a Cartesian (planar) coordinate system onto a cylindrical coordinate system. The prism *X*, *Y*, and *Z* axes represent the axes along which translations are measured for knees and ankles under our new convention: movement of the distal ACS origin along *X* now represents pure joint distraction–compression, along *Y* now represents pure anterior–posterior translation, and along *Z* represents medial–lateral translation, regardless of the joint's flexion–extension rotation.

2.2 | Osteological ROM measurement

After collecting the true mobility data, we simulated paleobiological estimation of joint ROM by conducting virtual ROM analyses based on skeletal elements alone. Using the micro-CT-derived mesh models generated during our XROMM analysis, we created a digital marionette for each right-sided joint in Maya 2020 (Autodesk) based on the same coordinate systems used for cadaveric joint pose

measurement. For hip joints, these marionettes were created following Manafzadeh and Padian (2018), and for hinge joints, we used a new prism-based forward kinematic rigging approach that allowed the direct input of hinge joint translations under our new measurement convention (Figure 2c,d; Method S1).

Although the majority of virtual ROM studies to date have estimated mobility by allowing motion in only one rotational degree of freedom at a time (e.g., Lai et al., 2018; Mallison, 2010a,b; Molnar et al., 2021; Nyakatura et al., 2015; Pierce et al., 2012), previous work on both humans and birds has demonstrated that the rotational degrees of freedom interact substantially (see discussions by Haering et al., 2014; Kambic et al., 2017a). In other words, the maxima and minima in all three rotational degrees of freedom are not reached simultaneously, causing the selection of rotational starting, "neutral," or "reference" pose to influence the results of joint mobility measurements (we briefly confirm this outcome for the guineafowl knee in Figure S1). We therefore consider allowing combinations of motions in all three rotational degrees of freedom to be the current field's best practice and thus chose to test the viability of 3D joint poses throughout this study. We animated both hip joints through all possible combinations of flexion–extension rotation = [−180,180], abduction–adduction rotation = [−90,90], and long-axis rotation = [−180,180] degrees at five-degree increments for a total of 197,173 rotational poses. Because hinge joints are presumably limited in rotation by their bicondylar morphology, we did not sample all possible rotational combinations, but instead animated each hinge joint through combinations of flexion–extension rotation = [0,180], abduction–adduction rotation = [−90,90], and long-axis rotation = [−90,90]° at five-degree increments for a total of 50,653 rotational poses. Such conservatively broad ranges were chosen to thoroughly sample pose space while avoiding arbitrary cutoff angles.

We then automatically assessed pose viability for each joint by calculating the Boolean intersection of the bone mesh models at every animation frame and taking its surface area (following Manafzadeh & Padian, 2018). If the bone mesh models did not interpenetrate, the Boolean intersection mesh had zero surface area, and the pose was classified as viable. After testing all possible rotational poses, the set of joint poses classified as viable was taken to represent the joint's rotational mobility (see "ROM Mapping" section). In this study, we estimated joint mobility under three different conditions with increasing translational degrees of freedom, referred to here as "no-translation," "single-translation," and "all-translation." We chose to set translations for all three conditions based on values obtained from our cadaveric ROM analysis. Given that such translation ranges are not known in paleobiological studies, our analyses represent a conservative best case scenario in which our simulations have the strongest possible chance of succeeding in capturing true joint mobility. A detailed protocol and code for the automatic incorporation of joint translations into the interpenetration detection workflow originally developed by Manafzadeh and Padian (2018) is provided as Method S2.

Under the no-translation approach, we held the joint rotational pivot in a fixed location (as done by Demuth et al., 2020; Lai et al., 2018; Mallison, 2010a,b; Nyakatura et al., 2015), with joint distraction–compression (Z translation at hip joints; X translation at hinge joints) set to the middle of the measured cadaveric range for each joint, and the other two translational degrees of freedom set to zero. The no-translation condition resulted in 197,173 hip joint configurations and 50,653 hinge joint configurations tested per joint. Under the single-translation approach, we allowed translation of the rotational pivot along the axis representing joint distraction–compression to the minimum, mid-range, and maximum values measured from cadavers to simulate pooling the results of joint space sensitivity analyses (e.g., those of Demuth et al., 2020; Nyakatura et al., 2015; and Richards et al., 2021). The single-translation condition evaluated three translations per rotational pose, resulting in 591,519 hip joint configurations and 151,959 hinge joint configurations tested per joint. Finally, under the all-translation approach, motions of the rotational pivot in all three translational degrees of freedom were allowed, again to the minimum, mid-range, and maximum values measured from cadavers, resulting in 27 ($3 \times 3 \times 3$) combinations of translations tested at each rotational pose. The all-translation condition resulted in 5,323,671 hip joint configurations and 1,367,631 hinge joint configurations tested per joint. To our knowledge, no virtual ROM study to date has systematically allowed combinations of motions in all three rotational and all three translational degrees of freedom (but see a partial six degree of freedom sensitivity analysis by Richards et al., 2021).

2.3 | ROM mapping

After measuring joint poses from both cadaveric manipulations and osteological simulations, we then assessed whether each simulation method successfully captured true joint rotational mobility—and in turn, would be reliable for use in ROM-based exclusion—by using ROM mapping (see Manafzadeh & Padian, 2018). For each joint studied, all possible cadaveric and osteological joint poses were plotted in cosine-corrected Euler joint pose space as 3D (cosine-corrected flexion–extension, abduction–adduction, long-axis rotation) points with central cosine-corrected flexion–extension (i.e., $\alpha_{central}$) set to 90° (following Manafzadeh & Gatesy, 2020; Manafzadeh et al., 2021). Cosine-corrected Euler space was used because it resolves the distortion inherent to uncorrected Euler space (e.g., Demuth et al., 2020; Haering et al., 2014; Kambic et al., 2017a; Manafzadeh & Padian, 2018; Richards et al., 2021) and allows quantitatively accurate comparisons of rotational mobility. We then virtually "shrink-wrapped" each joint pose point cloud (cadaveric, no-translation, single-translation, and all-translation) by calculating its alpha shape using MATLAB_R2019a (Mathworks), yielding polygonal envelopes representing both true and estimated mobilities. All alpha shapes were calculated using an alpha radius

of 10 or the critical alpha value, whichever was greater, following Manafzadeh and Gatesy (2020).

Alpha shapes were exported from MATLAB as OBJ files and imported into Maya for visual comparison in a common joint pose space. In order to quantitatively evaluate the reliability of osteological ROM estimates for use in ROM-based exclusion, we calculated the volume of each alpha shape in MATLAB. In any case where an osteological ROM estimate failed to capture all possible intact cadaveric poses, the percentage of true ROM that it failed to capture was calculated by subtracting the volume of the intersection of true and estimated ROM from the volume of true ROM and dividing the result by the volume of true ROM.

3 | RESULTS

3.1 | Cadaveric manipulations

Our cadaveric manipulations of guineafowl and alligator hindlimbs allowed us to generate alpha shapes representing the true rotational mobility of each joint. The volumes of these alpha shapes are reported in Table 1.

Our calculations of six degree of freedom kinematics revealed that all joints studied undergo excursions in all three translational degrees of freedom while assuming their full set of rotational poses (Table 2). We observed substantial interactions among these translational degrees of freedom, analogous to the interactions previously observed among rotational degrees of freedom by Haering et al., (2014), Kambic et al., (2017a), and others. In other words, the maxima and minima in all three translational degrees of freedom were never reached simultaneously (Figure S2).

3.2 | No-translation estimation

We conducted our three osteological simulations in the order of increasing complexity (no-translation, single-translation, all-translation). We present the results of these simulations as Figure 3 and Movies S2–6.

Volumes of alpha shapes obtained under the no-translation condition are reported in Table 1. All of these volumes exceed their corresponding true mobility volumes, but only the alligator hip no-translation simulation succeeded in capturing all rotational poses in the true cadaveric ROM (Figure 3a). Despite setting each joint's distraction–compression translation to the middle of its cadaveric range, the guineafowl hip, knee, and ankle and alligator knee simulations failed to capture 14, 42, 62, and 89 percent of cadaveric mobility, respectively, including many poses used in life by both animals during steady forward locomotion and non-locomotor behaviors (Manafzadeh et al., 2021; Figure S3).

That said, it is critical to note that this single rotational pivot position only succeeded in capturing alligator hip mobility because we input a sufficiently large value for joint distraction–compression translation into our digital marionette (i.e., sufficiently translated

TABLE 1 Volumes of alpha shapes for true and estimated joint mobilities, in cubic degrees

	Cadaveric (True)	No-translation	Single-translation	All-translation
Guineafowl Hip	34,037	549,195	1,284,989	1,386,601
Guineafowl Knee	43,757	340,846	1,771,992	3,628,433
Guineafowl Ankle	18,506	19,550	997,911	2,549,450
Alligator Hip	531,999	8,870,394	10,414,280	12,426,236
Alligator Knee	216,612	233,966	2,299,991	3,706,035

Note: Note that although all three estimated joint mobilities are larger than the true mobility for each joint, many simulations still fail to capture some of the rotational poses reached in manipulations of intact cadavers (Figure 3).

TABLE 2 Minimum and maximum excursions measured in each translational degree of freedom from each studied joint, in centimeters

	Guineafowl Hip		Guineafowl Knee		Guineafowl Ankle		Alligator Hip		Alligator Knee	
Translation	Min	Max	Min	Max	Min	Max	Min	Max	Min	Max
X	−0.056	0.203	0.309	0.983	0.398	0.692	−0.367	0.448	0.000	1.034
Y	−0.108	0.149	−0.343	0.934	−0.242	0.526	−0.492	0.897	−0.113	1.144
Z	−0.216	0.057	−0.398	0.297	−0.138	0.138	−0.749	0.040	−0.046	0.658

Measurement conventions for both hip joints follow previous XROMM studies, whereas knee and ankle measurements follow the prism-based hinge joint convention presented in this study. All values reflect right-sided conventions for positive measurements. See Kambic et al., (2014) for hip joint conventions; for knee joints, right-sided positive *X* represents joint distraction, positive *Y* represents relative anterior motion of the distal element, and positive *Z* represents relative lateral motion of the distal element; for the ankle joint, right-sided positive *X* represents joint distraction, positive *Y* represents relative posterior motion of the distal element, and positive *Z* represents relative medial motion of the distal element (see Method S1)

the femoral head out of the acetabulum), informed by our cadaveric manipulation data. When we conducted a subsequent sensitivity analysis (see Figure S4; Movie S7) and halved this translational value, the resulting simulation still succeeded in capturing cadaveric mobility. However, when we instead used a single pivot position determined by superimposing the best-fit spheres used to develop our joint coordinate systems (i.e., zero translation; see Kambic et al., 2014; cf. Demuth et al,l.,l., 2020; Manafzadeh & Padian, 2018; Nyakatura et al., 2015), the osteological estimation failed to capture 80 percent of cadaveric mobility. This outcome confirms that paleobiological estimates of ROM are highly sensitive to the distraction–compression placement of the joint rotational pivot, meaning that different "cartilage correction factors" (see Holliday et al., 2010) can produce very different results (see also sensitivity analyses by Demuth et al., 2020; Nyakatura et al., 2015; and Richards et al., 2021).

3.3 | Single-translation estimation

Volumes of alpha shapes obtained under the single-translation condition are reported in Table 1. With the addition of this translational degree of freedom, the guineafowl hip simulation also succeeded in capturing true cadaveric ROM (Figure 3b). However, the simulations for all three hinge joints—the guineafowl knee and ankle and alligator knee—still failed to capture 6, 12, and 3 percent of cadaveric mobility, respectively, including many poses used in life at the guineafowl ankle during steady forward locomotion and by both animals during non-locomotor behaviors (Manafzadeh et al., 2021; Figure S3). In other words, paleobiological estimates of ROM that include only a single translational degree of freedom in the form of a joint spacing or cartilage correction range would still fail to capture the full true mobility of these joints.

3.4 | All-translation estimation

With all three translational degrees of freedom allowed, our simulations successfully captured the true cadaveric ROM of all five joints (Figure 3). Note that the 180° flexion–extension rotation range we prescribed for hinge joints was surprisingly insufficient to capture all cadaveric guineafowl ankle poses, but when we allowed an additional five degrees of joint extension, all poses were captured (0.25% of volume originally missed; see Figure S5; Movie S8). Final alpha shape volumes for the all-translation condition are reported in Table 1.

Although our all-translation simulations succeeded in capturing true mobility, the resulting volumes for the guineafowl hip, knee, and ankle and alligator hip and knee overestimate true mobility by more than an order of magnitude (41, 83, 138, 23, and 17 times, respectively). In fact, they comprise 9.6, 97.8, 66.9, 86.0, and 99.9 percent of the full region of pose space sampled. It is thus likely that when all six degrees of freedom are allowed, very few joint poses can be excluded based on bone-on-bone interpenetration alone—unless the joint is extremely osteologically constrained, such as the guineafowl hip—highlighting the need for additional pose viability criteria (cf. Molnar et al., 2021; Pierce et al., 2012; Richards et al., 2021; see Discussion).

4 | DISCUSSION

ROM-based exclusion of impossible joint poses has long been a cornerstone of paleobiological reconstructions of functional anatomy, but we conclude that it requires a fundamental revision to become a reliable practice. Contrary to conventional wisdom, osteological estimates of ROM are not necessarily sweeping overestimates of true mobility. Our analyses reveal that these estimates may succeed in capturing all intact cadaveric joint poses either (a) with no translation allowed, (b) with translation allowed in distraction–compression, or (c) only when all three translational degrees of freedom are allowed (Figure 3). Because it is impossible to know which of these three outcomes will hold true for any given fossil joint and because these results are so sensitive to the initial placement of a joint's rotational pivot (Figure S4), which in any single fixed position cannot replicate a migrating instantaneous center of rotation (e.g., Aiyangar et al., 2017; Imaeda et al., 1996), we contend that all six degrees of freedom must be included in virtual ROM analyses to ensure that viable joint poses are not inadvertently excluded.

We therefore suggest that existing paleobiological studies founded on ROM-based exclusion be revisited to determine whether their functional and evolutionary conclusions are still supported when combinations of both rotational and translational degrees of freedom are allowed. This re-evaluation is especially critical for studies that have shaped our understanding of locomotor evolution. Likewise, we contend that future ROM estimation studies must allow combinations of rotational degrees of freedom and should explore the effects of translations with sensitivity analyses, taking only the most conservative results into account when excluding poses from reconstructions. We offer paleobiologists the tools necessary to automate six degree of freedom ROM analyses as Methods S1–2

FIGURE 3 Osteological ROM estimation can result in three potential outcomes. Analyses may succeed in capturing true mobility (a) with no translation allowed, (b) with just distraction–compression translation, or (c–e) only with all three translational degrees of freedom. Rotational mobility results for no-translation, single-translation, and all-translation simulations are displayed for the (a) alligator hip, (b) guineafowl hip, (c) guineafowl knee, (d) guineafowl knee, and (e) alligator knee as colored, transparent polygonal envelopes. Bolded gridlines represent 0 degrees; gridlines are 15 degrees apart. Axis orientation is in the upper left where FE_{CC} = cosine-corrected flexion–extension rotation, $ABAD_{CC}$ = cosine-corrected abduction–adduction rotation, and LAR_{CC} = cosine-corrected long-axis rotation. Alpha shapes representing the true cadaveric mobility of each joint are displayed in opaque gray. If true mobility was not captured, missed regions are highlighted in red, the simulation alpha shape is yellow, and the percent missed is reported; if true mobility was successfully captured, the simulation alpha shape is green. See also Movies S2–6

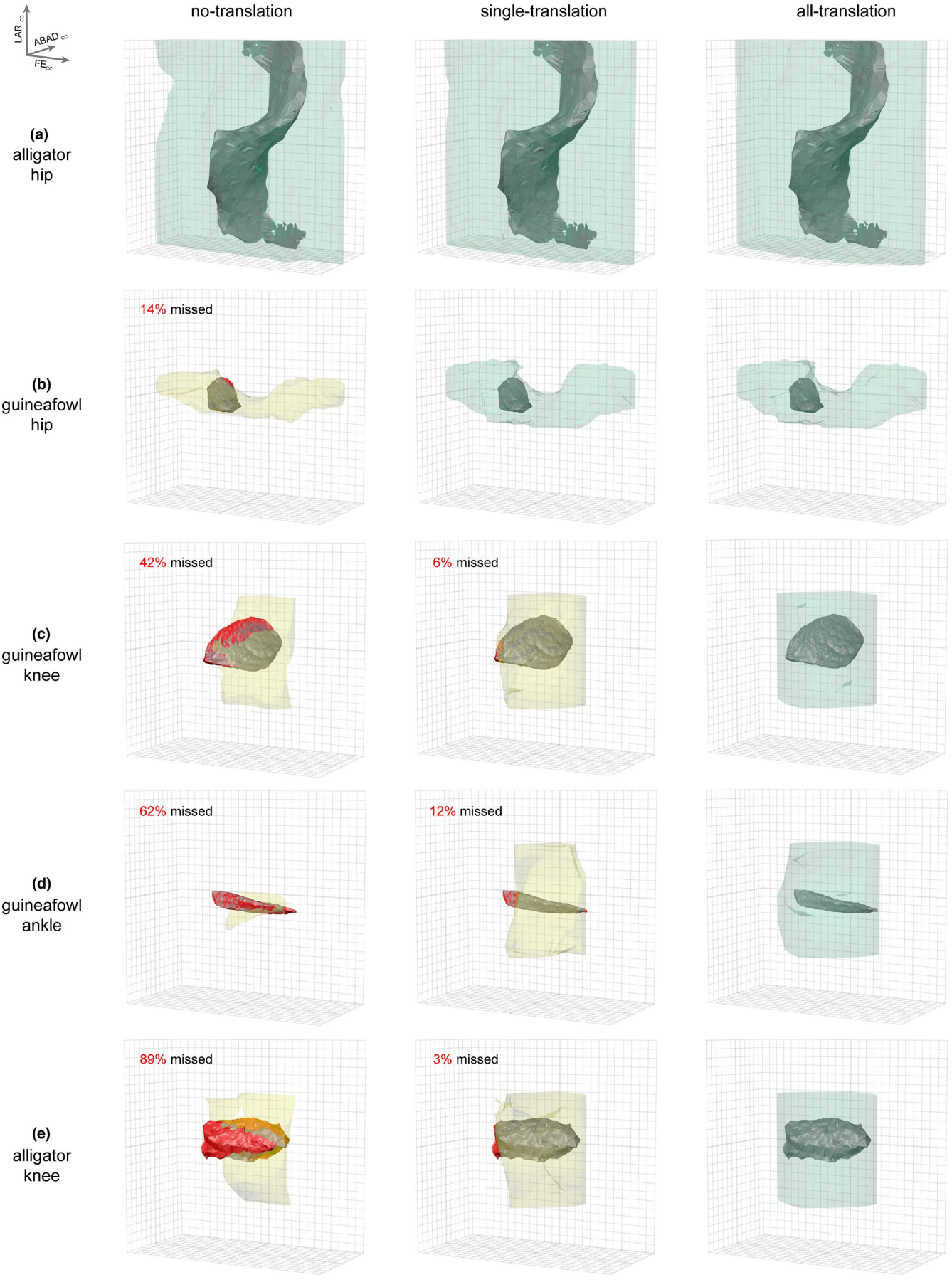
no-translation
single-translation
all-translation
LAR cc
ABAD cc
FE cc
(a) alligator hip
(b) guineafowl hip
14% missed
(c) guineafowl knee
42% missed
6% missed
(d) guineafowl ankle
62% missed
12% missed
(e) alligator knee
89% missed
3% missed

in the hope of facilitating and expediting both the reanalysis of existing studies and the initiation of new ones.

That said, our all-translation simulations indicate that once all six degrees of freedom are allowed, very few joint poses might appear impossible (as little as 0.1%)—precluding meaningful ROM-based exclusion, and arguably even defeating the purpose of ROM estimation. How, then, can we balance our competing needs for ROM estimates that are reliable (no erroneous exclusion) and yet informative (sufficient accurate exclusion)? We suggest that the answer lies in exploring how interactions among all six degrees of freedom work together to produce joint motion, and how these interactions are reflected in the dynamic morphological relationships of mating articular surfaces. Several ROM studies to date have incorporated an "articulation" criterion to eliminate poses when articular surfaces fail to achieve a certain percentage of overlap (e.g., Molnar et al., 2021; Pierce et al., 2012) or when mating bones move too far apart (e.g., Richards et al., 2021). We propose that by collecting data from living animals to assess and refine articulation criteria for disparate joints (e.g., Cobley et al., 2013; Jenkins & Camazine, 1977; Kambic et al., 2017b; Tsai et al., 2020), paleobiologists can then harness them to reliably whittle down future six degree of freedom ROM estimates without erroneously omitting viable poses. As articulation criteria are discovered, formalized, and validated, they can easily be layered onto the methodological framework we present here.

We suspect that until these criteria are identified, the inclusion of all six degrees of freedom will weaken or invalidate many existing functional interpretations and, as a result, may generate skepticism about the power of paleobiological inference. However, we emphasize that this outcome does not insinuate that the reconstruction of organismal function is a misbegotten endeavor. Rather, we hope that it will underscore the importance of developing a more nuanced understanding of proper articulation and serve as a motivator, shifting the focus of ROM analysis and ultimately increasing the rigor of future paleobiological investigations.

There is no question that ROM analyses have the potential to contribute extremely valuable data to paleobiological reconstructions of organismal function. In addition to their long-appreciated role in ROM-based exclusion, comparative mobility data have recently been found to help reveal which joint poses animals use during locomotion (Manafzadeh et al., 2021). However, in order to ensure that the inferences drawn from mobility data are accurate, we must continue to ground-truth our assumptions and test the validity of our ROM estimation methods using data from the joints of living animals. As we continue to refine our estimates of joint mobility and integrate them with other anatomical, kinetic, and kinematic lines of evidence (e.g., Bishop et al., 2021; Carrano et al., 1998; Molnar et al., 2021; Nyakatura et al., 2019), we will be better positioned to reconstruct not only individual extinct animals but also major functional transformations in vertebrate evolution.

ACKNOWLEDGMENTS

The authors thank David Baier for the XROMM_MayaTools package; John Hermanson, Sterling Nesbitt, Tomasz Owerkowicz, Karyn Roorda, and Michelle Stocker for supplying cadavers; Jeremy Lomax for assistance with cadaveric data collection; and Peter Bishop and an anonymous reviewer for their constructive feedback. This work was supported by the Bushnell Research and Education Fund, US National Science Foundation (Grants IOS-0925077, DBI-0552051, IOS-0840950, DBI-1262156, EAR-1452119, GRFP), Sigma Xi Grant-in-Aid of Research, Society of Vertebrate Paleontology Cohen Award for Student Research, Association of Women Geoscientists/Paleontological Society Winifred Goldring Award, and Brown University Presidential Fellowship.

AUTHOR CONTRIBUTIONS

Both authors designed research, performed research, analyzed data, and wrote, edited, and approved the manuscript.

DATA AVAILABILITY STATEMENT

All calibration images, X-ray videos, and CT files have been deposited in the X-ray Motion Analysis Research Portal (xmaportal.org; Study Identifiers BROWN20, BROWN58, and BROWN71) and are publicly available.

ORCID

Armita R. Manafzadeh https://orcid.org/0000-0001-5388-7942

REFERENCES

Aiyangar, A., **Zheng**, L., **Anderst**, W. & Zhang, X. (2017) Instantaneous centers of rotation for lumbar segmental extension in vivo. *Journal of Biomechanics*, 52, 113–121.

Arnold, P., **Fischer**, M.S. & **Nyakatura**, J.A. (2014) Soft tissue influence on *ex vivo* mobility in the hip of *Iguana*: Comparison with in vivo movement and its bearing on joint motion of fossil sprawling tetrapods. *Journal of Anatomy*, 225, 31–41.

Bishop, P.J., **Cuff**, A.R. & **Hutchinson**, J.R. (2021) How to build a dinosaur: Musculoskeletal modeling and simulation of locomotor biomechanics in extinct animals. *Paleobiology*, 47, 1–38.

Brainerd, E.L., **Baier**, D.B., **Gatesy**, S.M., Hedrick, T.L., Metzger, K.A., Gilbert, S.L. & et al. (2010) X-ray reconstruction of moving morphology (XROMM): precision, accuracy and applications in comparative biomechanics research. *Journal of Experimental Zoology Part A: Ecological Genetics and Physiology*, 313, 262–279.

Bramwell, C.D. & **Whitfield**, G.R. (1974) Biomechanics of *Pteranodon*. *Philosophical Transactions of The Royal Society London B*, 267, 503–581.

Camp, A.L. & **Brainerd**, E.L. (2014) Role of axial muscles in powering mouth expansion during suction feeding in largemouth bass (*Micropterus salmoides*). *Journal of Experimental Biology*, 217, 1333–1345.

Carpenter, K. (2002) Forelimb biomechanics of nonavian theropod dinosaurs in predation. *Senckenbergiana lethaea*, 82, 59–75.

Carpenter, K. & **Wilson**, Y. (2008) A new species of *Camptosaurus* (Ornithopoda: Dinosauria) from the Morrison Formation (Upper Jurassic) of Dinosaur National Monument, Utah, and a biomechanical analysis of its forelimb. *Annals of Carnegie Museum*, 76, 227–263.

Carrano, M.T. (1998) Locomotion in non-avian dinosaurs: Integrating data from hindlimb kinematics, in vivo strains, and bone morphology. *Paleobiology*, 24, 450–469.

Cobley, M.J., **Rayfield**, E.J. & **Barrett**, P.M. (2013) Inter-vertebral flexibility of the ostrich neck: implications for estimating sauropod neck flexibility. *PLoS One*, 8, e72187.

Dawson, M.M., **Metzger**, K.A., **Baier**, D.B. & Brainerd, E.L. (2011) Kinematics of the quadrate bone during feeding in mallard ducks. *Journal of Experimental Biology*, 214, 2036–2046.

Demuth, O.E., **Rayfield**, E.J. & **Hutchinson**, J.R. (2020) 3D hindlimb joint mobility of the stem-archosaur *Euparkeria capensis* with implications for postural evolution within Archosauria. *Scientific Reports*, 10, 1–14.

Fröbisch, J. (2006) Locomotion in derived dicynodonts (Synapsida, Anomodontia): a functional analysis of the pelvic girdle and hind limb of *Tetragonias njalilus*. *Canadian Journal of Earth Sciences*, 43, 1297–1308.

Gatesy, S.M., **Bäker**, M. & **Hutchinson**, J.R. (2009) Constraint-based exclusion of limb poses for reconstructing theropod dinosaur locomotion. *Journal of Vertebrate Paleontology*, 29, 535–544.

Grood, E.S. & **Suntay**, W.J. (1983) A joint coordinate system for the clinical description of three-dimensional motions: Application to the knee. *Journal of Biomechanical Engineering*, 105, 136–144.

Haering, D., **Raison**, M. & **Begon**, M. (2014) Measurement and description of three-dimensional shoulder range of motion with degrees of freedom interactions. *Journal of Biomechanical Engineering*, 136, 084502.

Holliday, C.M., **Ridgely**, R.C., **Sedlmayr**, J.C. et al. (2010) Cartilaginous epiphyses in extant archosaurs and their implications for reconstruction limb function in dinosaurs. *PLoS One*, 5, e13120.

Hutson, J.D. & **Hutson**, K.N. (2012) A test of the validity of range of motion studies of fossil archosaur elbow mobility using repeated-measures analysis and the extant phylogenetic bracket. *Journal of Experimental Biology*, 215, 2030–2038.

Hutson, J.D. & **Hutson**, K.N. (2013) Using the American alligator and a repeated measures design to place constraints on *in vivo* shoulder joint range of motion in dinosaurs and other fossil archosaurs. *Journal of Experimental Biology*, 216, 275–284.

Hutson, J.D. & **Hutson**, K.N. (2014) A repeated-measures analysis of the effects of soft tissues on wrist range of motion in the extant phylogenetic bracket of dinosaurs: Implications for the functional origins of an automatic wrist folding mechanism in *Crocodilia*. *Anatomical Record*, 297, 1228–1249.

Hutson, J.D. & **Hutson**, K.N. (2015) Inferring the prevalence and function of finger hyperextension in Archosauria from finger-joint range of motion in the American alligator. *Journal of Zoology*, 296, 189–199.

Imaeda, T., **Cooney**, W.P., **Niebur**, G.L., Linscheid, R.L. & An, K.-N. (1996) Kinematics of the trapeziometacarpal joint: A biomechanical analysis comparing tendon interposition arthroplasty and total-joint arthroplasty. *The Journal of Hand Surgery*, 21, 544–553.

Jenkins, F.A. (1971) The postcranial skeleton of African cynodonts. *Bulletin of the Peabody Museum of Natural History*, 36, 1–216.

Jenkins, F.A. & **Camazine**, S.M. (1977) Hip structure and locomotion in ambulatory and cursorial carnivores. *Journal of Zoology*, 181, 351–370.

Kambic, R.E., **Biewener**, A.A. & **Pierce**, S.E. (2017b) Experimental determination of three-dimensional cervical joint mobility in the avian neck. *Frontiers in Zoology*, 14, 1–15.

Kambic, R.E., **Roberts**, T.J. & **Gatesy**, S.M. (2014) Long-axis rotation: A missing degree of freedom in avian bipedal locomotion. *Journal of Experimental Biology*, 217, 2770–2782.

Kambic, R.E., **Roberts**, T.J. & **Gatesy**, S.M. (2017a) 3-D range of motion envelopes reveal interacting degrees of freedom in avian hind limb joints. *Journal of Anatomy*, 231, 906–920.

Knörlein, B.J., **Baier**, D.B., **Gatesy**, S.M. et al. (2016) Validation of XMALab software for marker-based XROMM. *Journal of Experimental Biology*, 219, 3701–3711.

Lai, P.H., **Biewener**, A.A. & **Pierce**, S.E. (2018) Three-dimensional mobility and muscle attachments in the pectoral limb of the Triassic cynodont *Massetognathus pascuali* (Romer, 1967). *Journal of Anatomy*, 62, 383–406.

Mallison, H. (2010a) CAD assessment of the posture and range of motion of *Kentrosaurus aethiopicus* Hennig 1915. *Swiss Journal of Geosciences*, 103, 211–233.

Mallison, H. (2010b) The digital *Plateosaurus* II: An assessment of the range of motion of the limbs and vertebral column and of previous reconstructions using a digital skeletal mount. *Acta Palaeontologica Polonica*, 55, 433–458.

Manafzadeh, A.R. (2020) A practical guide to measuring ex vivo joint mobility using XROMM. *Integrative Organismal Biology*, 2, obaa041.

Manafzadeh, A.R. & **Gatesy**, S.M. (2020) A coordinate-system-independent method for comparing joint rotational mobilities. *Journal of Experimental Biology*, 223, jeb227108.

Manafzadeh, A.R., **Kambic**, R.E. & **Gatesy**, S.M. (2021) A new role for joint mobility in reconstructing vertebrate locomotor evolution. *Proceedings of the National Academy of Sciences*, 118, e2023513118.

Manafzadeh, A.R. & **Padian**, K. (2018) ROM mapping of ligamentous constraints on avian hip mobility: Implications for extinct ornithodirans. *Proceedings of the Royal Society B: Biological Sciences*, 285, 20180727.

Menegaz, R.A., **Baier**, D.B., **Metzger**, K.A. et al. (2015) XROMM analysis of tooth occlusion and temporomandibular joint kinematics during feeding in juvenile miniature pigs. *Journal of Experimental Biology*, 218, 2573–2584.

Molnar, J.L., **Hutchinson**, J.R., **Diogo**, R. et al. (2021) Evolution of forelimb musculoskeletal function across the fish-to-tetrapod transition. *Science Advances*, 7, eabd7457.

Nyakatura, J.A., **Allen**, V.R., **Lauströer**, J., Andikfar, A., Danczak, M., Ullrich, H.-J. et al. (2015) A three-dimensional skeletal reconstruction of the stem amniote *Orobates pabsti* (Diadectidae): Analyses of body mass, centre of mass position, and joint mobility. *PLoS One*, 10, e0137284.

Nyakatura, J.A., **Melo**, K., **Horvat**, T., Karakasiliotis, K., Allen, V.R., Andikfar, A. et al. (2019) Reverse-engineering the locomotion of a stem amniote. *Nature*, 565, 351–355.

Padian, K. (1983) A functional analysis of flying and walking in pterosaurs. *Paleobiology*, 9, 218–239.

Paul, G.S. & **Christiansen**, P. (2000) Forelimb posture in neoceratopsian dinosaurs: implications for gait and locomotion. *Paleobiology*, 26, 450–465.

Pierce, S.E., **Clack**, J.A. & **Hutchinson**, J.R. (2012) Three-dimensional limb joint mobility in the early tetrapod *Ichthyostega*. *Nature*, 486, 523–526.

Richards, H.L., **Bishop**, P.J., **Hocking**, D.P., Adams, J.W. & Evans, A.R. (2021) Low elbow mobility indicates unique forelimb posture and function in a giant extinct marsupial. *Journal of Anatomy*, 238, 1425–1441.

Senter, P. & **Robins**, J.H. (2005) Range of motion in the forelimb of the theropod dinosaur *Acrocanthosaurus atokensis*, and implications for predatory behaviour. *Journal of Zoology*, 266, 307–318.

Senter, P. & **Sullivan**, C.R. (2019) Forelimbs of the theropod dinosaur *Dilophosaurus wetherilli*: Range of motion, influence of paleopathology and soft tissues, and description of a distal carpal bone. *Palaeontologia Electronica*, 22, 1–9.

Thomason, J. (Ed.) (1995) *Functional morphology in vertebrate paleontology*. New York, NY: Cambridge University Press.

Tsai, H.P., **Turner**, M.L., **Manafzadeh**, A.R. et al. (2020) Contrast-enhanced XROMM reveals in vivo soft tissue interactions in the hip of *Alligator mississippiensis*. *Journal of Anatomy*, 236, 288–304.

SUPPORTING INFORMATION

Additional supporting information may be found online in the Supporting Information section.

How to cite this article: Manafzadeh, A.R. & Gatesy, S.M. (2021) Paleobiological reconstructions of articular function require all six degrees of freedom. *Journal of Anatomy*, 239, 1516–1524. https://doi.org/10.1111/joa.13513